

Half-awake to the risk of predation

Birds have overcome the problem of sleeping in risky situations by developing the ability to sleep with one eye open and one hemisphere of the brain awake¹. Such unihemispheric slow-wave sleep is in direct contrast to the typical situation in which sleep and wakefulness are mutually exclusive states of the whole brain. We have found that birds can detect approaching predators during unihemispheric slow-wave sleep, and that they can increase their use of unihemispheric sleep as the risk of predation increases. We believe this is the first evidence for an animal behaviourally controlling sleep and wakefulness simultaneously in different regions of the brain.

The function of unihemispheric slow-wave sleep (USWS) in birds has been unclear¹. In aquatic mammals — the only other group of animals known to exhibit USWS — this sleep pattern seems to allow concurrent sleep and surfacing to breathe². If avian USWS functions as a form of predator detection, then birds should be able to control whether they sleep primarily with one or both hemispheres in response to changes in predation risk³. Under safe conditions, birds can sleep more efficiently by sleeping with both hemispheres simultaneously, whereas under dangerous conditions a bird should increase USWS to remain vigilant for predators. Moreover, during USWS a bird should sleep with its open eye towards the direction from which a potential predator is likely to approach.

To test these expectations, we took advantage of the 'group edge effect', a phenomenon in which animals at the more risky edge of a group spend more time scanning visually for predators than those nearer the group's centre⁴. We predicted that birds sleeping at the edge of a group would spend more time in USWS, and would direct their open eye away from the group's centre towards potential predators.

We established four groups of mallard ducks (*Anas platyrhynchos*), each containing four individuals. Video recordings of sleep behaviour were made with the birds arranged in a row. Birds at the ends of the row (the edge of the group) were in a more exposed position than those in the central positions. The closure of one eye indicated USWS¹, whereas closing both eyes indicated either bihemispheric slow-wave sleep or rapid-eye-movement (REM) sleep, which occurs bihemispherically in birds⁵.

We found that mallards markedly increased their use of USWS when sleeping at the edge of the group. The proportion of sleep composed of USWS increased from $12.4 \pm 1.1\%$ (mean \pm s.e.) in the central position to $31.8 \pm 3.6\%$ in the edge position

(Wilcoxon matched-pairs signed-ranks test, $T=1$, $P<0.001$), an increase of more than 150%. Furthermore, birds in USWS at the edge position oriented the open eye away from the group's centre $86.2 \pm 3.1\%$ of the time (t -test, $t=11.58$, d.f. = 15, $P<0.001$), whereas birds in the central position showed no preference for gaze direction (time looking away, $52.8 \pm 3.7\%$; t -test, $t=0.76$, d.f. = 15, n.s.). Mallards therefore exhibited behavioural control of USWS and used it adaptively by looking in the direction of a potential threat.

Electroencephalographic (EEG) recordings obtained under the above conditions

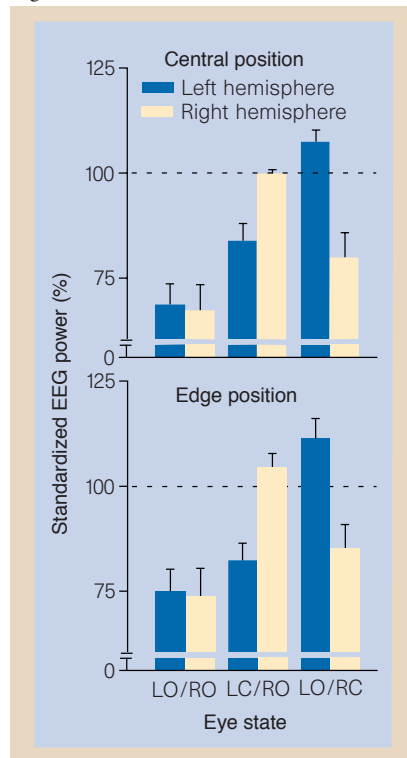


Figure 1 The relation between eye state and standardized EEG power (1–6 Hz) for the left and right hemispheres of birds occupying central and edge positions. EEGs were recorded from the dorsal surface of the hyperstriatum accessorium of each hemisphere, the part of the avian brain that most clearly reflects sleep-related changes in brain state⁵. The three eye states are: both left and right eyes open (LO/RO); left eye closed and right eye open (LC/RO); and left eye open and right eye closed (LO/RC). For each mallard ($n=6$), EEG power was standardized as a percentage of the average power observed during bihemispheric slow-wave sleep for each bird's hemisphere, so the broken line at 100% indicates EEG power equivalent to that during bihemispheric slow-wave sleep. Greater power in the hemisphere opposite the closed eye during unilateral eye closure indicates USWS. Further methodological details are available from the authors.

corroborated at the neurophysiological level our behavioural results. During each eye state, EEG recordings from each hemisphere were evaluated by digital period amplitude analysis, which quantifies the power (a measure of wave amplitude) of different frequencies within the EEG⁶. Avian slow-wave sleep is characterized by high power in the low-frequency range (1–6 Hz), whereas wakefulness is characterized by low power in this range⁵.

When one eye was closed, low-frequency power in the hemisphere opposite the closed eye (the sleeping hemisphere) was significantly greater than that in the hemisphere opposite the open eye ($T \leq 1$, $P < 0.05$ for all comparisons; Fig. 1), regardless of the position occupied by a bird, which confirms USWS. Low-frequency power in the awake hemisphere (that opposite the open eye) was nevertheless significantly greater than the power with both eyes open ($T=0$, $P < 0.05$ for all comparisons), indicating a quiet waking state intermediate between full alertness and slow-wave sleep. Subsequent tests confirmed that the waking hemisphere was capable of predator detection: mallards in USWS initiated escape behaviour within only 0.165 ± 0.006 seconds ($n=10$ mallards) of an expanding video image being presented, simulating predatory attack.

The EEG recordings confirmed that the 150% increase in unilateral eye closure was a direct result of an equivalent increase in the proportion of slow-wave sleep composed of USWS. Because bihemispheric slow-wave sleep and REM sleep both occur with both eyes closed, it was possible that a selective decrease in REM sleep in the edge position may have confounded our interpretation of the behavioural results. However, EEG analyses showed an almost 1:1 relation between unilateral eye closure and the proportion of slow-wave sleep composed of USWS. An increase in unilateral eye closure therefore reflected an equivalent increase in USWS.

A bird's ability to control sleep and wakefulness independently in each hemisphere is in accord with evidence indicating that each eye⁷ and associated hemisphere⁸ can function independently during wakefulness in birds. The neuroanatomical structures and physiological processes that allow independent hemispheric functioning during wakefulness may therefore also allow for the independent hemispherical control of sleep. The ability to control USWS behaviourally in response to changes in predation risk emphasizes the dynamic balance that animals must achieve between the ecological consequences and the physiological necessity of sleep⁹.

Niels C. Rattenborg, Steven L. Lima, Charles J. Amlaner

Department of Life Sciences,
Indiana State University,
Terre Haute, Indiana 47809, USA
e-mail: lsratten@scifac.indstate.edu

- Ball, N. J., Amlaner, C. J., Shaffery, J. P. & Opp, M. R. in *Sleep '86* (eds Koella, W. P., Obál, F., Schulz, H. & Visser, P.) 151–153 (Fischer, New York, 1988).
- Oleksenko, A. I., Mukhametov, L. M., Polyakova, I. G., Supin, A. Y. & Kovalzon, V. M. *J. Sleep Res.* **1**, 40–44 (1992).
- Lima, S. L. *Adv. Study Behav.* **27**, 215–290 (1998).
- Elgar, M. A. *Biol. Rev.* **64**, 13–33 (1989).
- Amlaner, C. J. & Ball, N. J. in *Principles and Practice of Sleep Medicine* 2nd edn (eds Kryger, M. H., Roth, T. & Dement, W. C.) 81–94 (Saunders, Philadelphia, 1994).
- Hoffmann, R. F., Moffitt, A. R., Shearer, J. C., Sussman, P. S. & Wells, R. B. *Waking Sleeping*, 3, 1–16 (1979).
- Schaeffel, F., Howland, H. C. & Farkas, L. *Vision Res.* **26**, 1977–1993 (1986).
- Bredenkötter, M. & Bischof, H.-J. *Vis. Neurosci.* **5**, 155–163 (1990).
- Rechtschaffen, A., Gilliland, M. A., Bergmann, B. M. & Winter, J. B. *Science* **221**, 182–184 (1983).

Pattern formation in semiconductors

In semiconductors, nonlinear generation and recombination processes of free carriers and nonlinear charge transport can give rise to non-equilibrium phase transitions^{1,2}. At low temperatures, the basic nonlinearity is due to the autocatalytic generation of free carriers by impact ionization of shallow impurities. The electric field accelerates free electrons, causing an abrupt increase in free carrier density at a critical electric field. In static electric fields, this nonlinearity is known to yield complex filamentary current patterns bound to electric contacts³.

We used microwaves to apply an electric field to semiconductor samples without using electrical contacts. High-frequency electric fields ionize impurities just as d.c. fields do⁴, but they do not impose inhomogeneities like electric contacts. We find that in thin n-type gallium arsenide (GaAs) epitaxial layers subjected to a uniform microwave field, circular spots of enhanced free electron density with sharp boundaries are spontaneously formed above a critical microwave threshold power. This new type of self-organized free-carrier density pattern is different from current filaments in that they are currentless; they also differ from electron-hole drops⁵ as only one type of charge carrier is involved.

The spatial patterns in free electron density were made visible by photoluminescence quenching⁶. Samples cooled to low temperatures (1.8 K) were illuminated by interband light and photographed in the spectral range of the luminescence of exciton recombination and donor–acceptor transitions. With increasing microwave power P , a decrease in photoluminescence occurs at a threshold value P_+ as a result of

an almost circular spot of enhanced electron density with a diameter (D_+) of about 1 mm (Fig. 1b). The diameter of the spot at the threshold is always finite and independent of the size of the semiconductor sample. This pattern formation was observed in doped samples with impurity densities of about 10^{15} per cm^3 , but not in ‘ultrapure’ material with an impurity density of about 5×10^{12} per cm^3 .

When the microwave power is increased above the threshold P_+ , the diameter of the original spot increases (Fig. 1b,c); at certain values of P , additional spots appear at a distance of 1 to 3 mm (Fig. 1d). Decreasing the microwave power after the first spot has formed makes it smaller until it vanishes at a power of $P_- < P_+$, at a diameter $D_- < D_+$ (Fig. 1e). The pattern formation process shows a hysteretic behaviour, as it is characteristic for a first-order phase transition.

The quenching of the photoluminescence in the spots indicates that the average energy of electrons is high enough to ionize impurities and excitons in the spots. The observed structures therefore correspond to spots of high free electron density. We verified this using a sample with two parallel stripe contacts at opposite edges. When a voltage was applied across the contacts, a current filament was formed in addition to the microwave-induced spot. The current filament goes through the spot, indicating that the observed structures are regions of high free electron density.

Our findings indicate that the physical background of microwave-induced pattern formation in the electron density is the

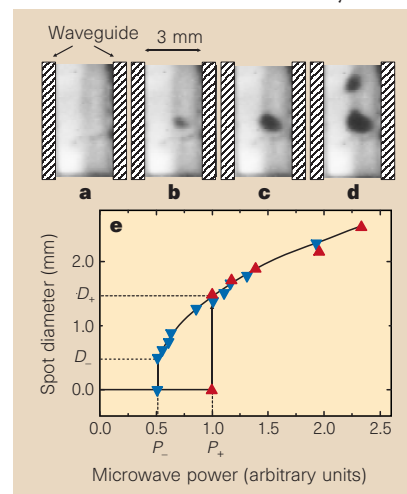


Figure 1 Self-organized formation of spots of high electron density in an n-doped gallium arsenide epitaxial layer as a result of impact ionization of shallow donors in a microwave electric field. **a–d**, Images of near-infrared luminescence for microwave power increasing from zero (**a**) to about 30 mW (**d**). Shaded stripes show the walls of a waveguide. **e**, Spot diameter as a function of microwave power. Red and blue triangles indicate increasing and decreasing power, respectively. P_+ is of the order of 10 mW.

same as that of current filamentation. Both of these phenomena are based on a bistability of conductivity combined with a constraint of the external driving mechanism. In the case of current filaments, the constraint is provided by the finite current applied to the sample, whereas for microwave-induced pattern formation the external constraint must be the limited power supply from the field.

Bistability and the possibility of spatial modulation of semiconductor conductivity have been attributed to three different physical mechanisms: multilevel generation and recombination kinetics of impurities², runaway of electron energy due to energy-dependent electron scattering⁷, and electron density-dependent screening of ionized impurity scattering⁴. For all three mechanisms, bistability vanishes below a critical density of impurities, which explains the qualitatively different behaviour of doped and ultrapure materials, for which pattern formation has not been observed.

V. V. Bel'kov*, J. Hirschinger*, V. Novák†, F.-J. Niedernostheide*, S.D. Ganichev*, W. Prettl*

*Institut für Experimentelle und Angewandte Physik, Universität Regensburg,
93040 Regensburg, Germany

†Institute of Electrical Engineering,
AV ČR, 182 02 Prague 8, Czech Republic
e-mail: wilhelm.prettl@physik.uni-regensburg.de

- Landsberg, P. T. & Pimpale, A. J. *Phys. C* **9**, 1243–1252 (1976).
- Schöll, E. *Nonequilibrium Phase Transitions in Semiconductors* (Springer, Berlin, 1987).
- Ridley, B. K. *Proc. Phys. Soc.* **82**, 954–966 (1963).
- Kozhevnikov, M. et al. *Phys. Rev. B* **52**, 4855–4863 (1995).
- Jeffries, C. D. *Science* **189**, 955–964 (1975).
- Eberle, W. et al. *Appl. Phys. Lett.* **68**, 3329–3331 (1996).
- Levinson, I. B. *Sov. Phys. Solid State* **7**, 1098–1102 (1965).

UV-B damage amplified by transposons in maize

While absorbing visible light energy for photosynthesis, plants are unavoidably exposed to ultraviolet radiation, which is particularly harmful at shorter wavelengths (UV-B radiation). Ozone depletion in the atmosphere means that plants receive episodic or steadily increasing doses of UV-B, which damages their photosynthetic reaction centres, crosslinks cellular proteins, and induces mutagenic DNA lesions¹. Plant adaptive mechanisms of shielding and repair are therefore critical to survival — for example, somatic tissues of maize and *Arabidopsis* defective in phenolic sunscreen pigments^{2,3} incur increased DNA damage, and mutants defective in DNA repair^{4,5} are killed by UV-B.

The harmful effects of UV-B on maize pollen are proportional to the exposure time⁶. I find that simulated field conditions